ARTICLE
Journal of Cellular Biochemistry 115:641–650 (2014)

Journal of Cellular Biochemistry

BRCA1-Mediated Inflammation and Growth Activated & Inhibited Transition Mechanisms Between No-Tumor Hepatitis/Cirrhotic Tissues and HCC

Haizhen Diao,[1,2] Lin Wang,[1,2*] Juxiang Huang,[1] Minghu Jiang,[3] Huilei Zhou,[1] Xiaohe Li,[1] Qingchun Chen,[1] Zhenfu Jiang,[4] and Haitao Feng[5]

[1]*Bioinformatics Center, School of Electronic Engineering, Beijing University of Posts and Telecommunications, Beijing 100876, China*

[2]*State key Laboratory of Drug Research, Shanghai Institute of Materia Medica, Chinese Academy of Sciences, Shanghai 201203, China*

[3]*Lab of Computational Linguistics, School of Humanities and Social Sciences, Tsinghua University, Beijing 100084, China*

[4]*School of Mechanical Electronic & Information Engineering, China University of Mining & Technology, Beijing 100083, China*

[5]*Heilongjiang University of Chinese Medicine, Harbin 150040, China*

ABSTRACT

To understand breast cancer 1 early onset (*BRCA1*)-mediated inflammation and growth activated and inhibited transition mechanisms between no-tumor hepatitis/cirrhotic tissues (HBV or HCV infection) and human hepatocellular carcinoma (HCC), *BRCA1*-activated different complete (all no positive correlation, Pearson correlation coefficient <0.25) and uncomplete (partly no positive correlation except *BRCA1*, Pearson <0.25) networks were identified in higher HCC compared with lower no-tumor hepatitis/cirrhotic tissues (HBV or HCV infection) from the corresponding *BRCA1*-stimulated (Pearson ≥ 0.25) or inhibited (Pearson ≤ -0.25) overlapping molecules of Pearson and GRNInfer, respectively. This result was verified by the corresponding scatter matrix. As visualized by GO, KEGG, GenMAPP, BioCarta, and disease database integration, we proposed mainly that *BRCA1*-stimulated different complete network was involved in *BRCA1* activation with integral to membrane killer cell lectin-like receptor C to nucleus interferon regulatory factor 5-induced inflammation, whereas the corresponding inhibited network participated in *BRCA1* repression with matrix roundabout axon guidance receptor homolog 1 to plasma membrane versican-induced growth in lower no-tumor hepatitis/cirrhotic tissues (HBV or HCV infection). However, *BRCA1*-stimulated network contained *BRCA1* activation with endothelium-specific to lysosomal transmembrane and carbamoyl synthetase to tastin, histone cluster and cyclin-induced growth, whereas the corresponding inhibited different complete network included *BRCA1* repression with ovalbumin, thyroid stimulating hormone beta and Hu antigen C to cytochrome P450 to transducin-induced inflammation in higher HCC. Our *BRCA1* different networks were verified by *BRCA1*-activated or -inhibited complete and uncomplete networks within and between no-tumor hepatitis/cirrhotic tissues (HBV or HCV infection) or (and) HCC. J. Cell. Biochem. 115: 641–650, 2014.

KEY WORDS: INFLAMMATION; GROWTH; BREAST CANCER 1 EARLY ONSET (*BRCA1*); HCC; NO-TUMOR HEPATITIS/CIRRHOTIC TISSUES (HBV OR HCV INFECTION)

Conflict of interest: None.

Haizhen Diao, Lin Wang, Juxiang Huang, and Minghu Jiang contributed equally to this work.

Grant sponsor: National Natural Science Foundation of China; Grant number: 61171114; Grant sponsor: State Key Laboratory of Drug Research; Grant number: SIMM1302KF; Grant sponsor: Automatical Scientific Planning of Tsinghua University; Grant numbers: 20111081023, 20111081010.

*Correspondence to: Prof. Lin Wang, Bioinformatics Center, School of Electronics Engineering, Beijing University of Posts and Telecommunications, Beijing 100876, China. Email: wanglin98@tsinghua.org.cn

Manuscript Received: 21 July 2013; Manuscript Accepted: 16 October 2013

Accepted manuscript online in Wiley Online Library (wileyonlinelibrary.com): 21 October 2013

DOI 10.1002/jcb.24699 • © 2013 Wiley Periodicals, Inc.

Breast cancer 1 early onset (*BRCA1*) is part of a complex that repairs double-strand breaks in DNA. The strands of the DNA double helix are continuously breaking from damage. Sometimes one strand is broken, and sometimes both strands are broken simultaneously. DNA cross linking agents are an important source of chromosome/DNA damage. Double strand breaks occur as intermediates after the cross links are removed. *BRCA1* is part of a protein complex that repairs DNA when both strands are broken. When both strands are broken, it is difficult for the repair mechanism to "know" how to replace the correct DNA sequence, and there are multiple ways to attempt the repair. This DNA repair takes place with the DNA in the cell nucleus, wrapped around the histone. Several proteins, including *BRCA1*, arrive at the histone-DNA complex for this repair. Regulatory aspect to *BRCA1* nuclear-non-nuclear distribution was first shown by Dr Rao laboratory in 1997 [Wang et al., 1997]. In the nucleus of many types of normal cells, the *BRCA1* protein interacts with RAD51 during repair of DNA double-strand breaks [Boulton, 2006]. These breaks can be caused by natural radiation or other exposures, but also occur when chromosomes exchange genetic material (homologous recombination, for example, "crossing over" during meiosis). Yet novel *BRCA1*-mediated inflammation and growth activated and inhibited transition mechanisms are not clear and remain to be elucidated between no-tumor hepatitis/cirrhotic tissues (HBV or HCV infection) and human hepatocellular carcinoma (HCC).

In the lower expression of no-tumor hepatitis/cirrhotic tissues (HBV or HCV infection), we detected 165 and 171 as *BRCA1*-activated and -inhibited targets for *BRCA1*-mediated inflammation and growth activated and inhibited transition mechanisms between no-tumor hepatitis/cirrhotic tissues (HBV or HCV infection) and HCC by GRNInfer (Table S1A), respectively. Validated 67 and 28 as *BRCA1*-activated (Pearson $\geq$0.25) and -inhibited (Pearson $\leq$−0.25) targets were also quantified for *BRCA1*-mediated inflammation and growth activated and inhibited transition mechanisms by Pearson analysis, respectively (Table S1B). 59 and 24 as *BRCA1*-activated and -inhibited targets were identified for *BRCA1*-mediated inflammation and growth activated and inhibited transition mechanisms by overlapping molecules of Pearson and GRNInfer, respectively (Table S1C). Taken together, the studies suggest that *BRCA1* includes maybe directly or indirectly at least potential 173 and 175 as *BRCA1*-activated and -inhibited distinct proteins for *BRCA1*-mediated inflammation and growth activated and inhibited transition mechanisms (Table S1D). Mutual 24 and 9 as *BRCA1*-activated and -inhibited targets were identified from overlapped analysis for *BRCA1*-mediated inflammation and growth activated and inhibited transition mechanisms by correlation coefficient, respectively (Table S1E). 2 of *BRCA1*-inhibited targets was selected as different mutual positive complete (all no positive correlation, Pearson <0.25) and 6 as uncomplete (partly no positive correlation except *BRCA1*, Pearson <0.25); 2 of *BRCA1*-activated targets as different mutual positive complete and 20 as uncomplete in lower no-tumor hepatitis/cirrhotic tissues (HBV or HCV infection) (compared with higher HCC) by Pearson analysis with fold changes seen (Table S1F,G,H).

In the higher expression of HCC, we detected 165 and 169 as *BRCA1*-activated and- inhibited targets for *BRCA1*-mediated inflammation and growth activated and inhibited transition mechanisms between no-tumor hepatitis/cirrhotic tissues (HBV or HCV infection) and HCC by GRNInfer (Table S1A), respectively. Validated 98 and 53 as *BRCA1*-activated (Pearson $\geq$0.25) and -inhibited (Pearson $\leq$−0.25) targets were also quantified for *BRCA1*-mediated inflammation and growth activated and inhibited transition mechanisms by Pearson analysis, respectively (Table S1B). 73 and 39 as *BRCA1*-activated and -inhibited targets were identified for *BRCA1*-mediated inflammation and growth activated and inhibited transition mechanisms by overlapping molecules of Pearson and GRNInfer, respectively (Table S1C). Taken together, the studies suggest that *BRCA1* includes maybe directly or indirectly at least potential 190 and 184 as *BRCA1*-activated and -inhibited distinct proteins for *BRCA1*-mediated inflammation and growth activated and inhibited transition mechanisms (Table S1D). Mutual 35 and 31 as *BRCA1*-activated and -inhibited targets were identified from overlapped analysis for different *BRCA1* networks for *BRCA1*-mediated inflammation and growth activated and inhibited transition mechanisms by correlation coefficient, respectively (Table S1E). Six of *BRCA1*-inhibited targets was selected as different mutual positive complete (all no positive correlation, Pearson <0.25) and 25 as uncomplete (partly no positive correlation except *BRCA1*, Pearson <0.25); 7 of *BRCA1*-activated targets as different mutual positive complete, and 19 as uncomplete in higher HCC (compared with lower no-tumor hepatitis/cirrhotic tissues (HBV or HCV infection)) by Pearson analysis with fold changes seen (Table S1F,G,H).

MATERIALS AND METHODS

Breast cancer 1 early onset (*BRCA1*) (our identified 225 significant molecules in 6,144 genes of 25 higher HCC) was identified from the corresponding 25 lower no-tumor hepatitis/cirrhotic tissues (HBV or HCV infection) in GEO data set GSE10140-10141 (http://www.ncbi.nlm.nih.gov/geo/query/acc.cgi?acc=GSE10140, http://www.ncbi.nlm.nih.gov/geo/query/acc.cgi?acc=GSE10141). The raw microarray data was processed by log base 2.

Novel *BRCA1*-activated (Pearson $\geq$0.25) and -inhibited (Pearson $\leq$−0.25) different networks were detected and quantified from 225 significant molecules between lower no-tumor hepatitis/cirrhotic tissues (HBV or HCV infection) and higher HCC using significant analysis of microarrays (SAM) (http://www-stat.stanford.edu/~tibs/SAM/) [Storey., 2002] and our programming. Two classes paired and minimum fold change $\geq$2 were selected (the false-discovery rate 0%).

Mutual relationships of novel *BRCA1*-activated (Pearson $\geq$0.25) and -inhibited (Pearson $\leq$−0.25) different complete (all no positive correlation, Pearson <0.25) and uncomplete (partly no positive correlation except *BRCA1*, Pearson <0.25) networks were computed between lower no-tumor hepatitis/cirrhotic tissues (HBV or HCV infection) and higher HCC by SPSS of Pearson correlation coefficient quantification about measures of the correlation (linear dependence) between two variables X and Y, giving a value between +1 and −1 inclusive and our programming, respectively.

Mutual relationships of novel *BRCA1*-activated (Pearson$\geq$ 0.25) and -inhibited (Pearson $\leq$−0.25) different complete (all no positive correlation, Pearson <0.25) and uncomplete (partly no positive

correlation except *BRCA1*, Pearson <0.25) networks were investigated between lower no-tumor hepatitis/cirrhotic tissues (HBV or HCV infection) and higher HCC by SPSS of scatterplot (matrix) based on linear regression and our programming, respectively.

Novel *BRCA1*-activated (Pearson ≥0.25) and -inhibited (Pearson ≤−0.25) different complete (all no positive correlation, Pearson <0.25) and uncomplete (partly no positive correlation except *BRCA1*, Pearson <0.25) networks were constructed between lower no-tumor hepatitis/cirrhotic tissues (HBV or HCV infection) and higher HCC by GRNInfer [Wang et al., 2006], our articles [Wang et al., 2009a, b, 2011a,b,c,d,e,f, 2012a,b,c,d; Huang et al., 2010, 2011, 2012; Sun et al., 2010; Sun et al., 2011; Lin et al., 2012] and GVedit tool and our programming, respectively.

Terms and occurrence numbers of GO (Cellular Component, Molecular Function, Biological Process), KEGG, GenMAPP, BioCarta, and disease in novel *BRCA1*-activated (Pearson ≥0.25) and -inhibited (Pearson ≤−0.25) different complete (all no positive correlation, Pearson <0.25) and uncomplete (partly no positive correlation except *BRCA1*, Pearson <0.25) networks were identified between lower no-tumor hepatitis/cirrhotic tissues (HBV or HCV infection) and higher HCC, respectively, by Molecule Annotation System, MAS (CapitalBio Corporation, Beijing, China; http://bioinfo.capitalbio.com/mas3/) and our programming. The primary databases of MAS integrated various well-known biological resources, such as Gene Ontology (http://www.geneontology.org), KEGG (http://www.genome.jp/kegg/), BioCarta (http://www.biocarta.com/), GenMapp (http://www.genmapp.org/), HPRD (http://www.hprd.org/), etc.

RESULT

Mutual relationships of novel *BRCA1*-activated (Pearson ≥0.25) and -inhibited (Pearson ≤−0.25) different complete and uncomplete networks grouped vertical bars quantification chart between lower no-tumor hepatitis/cirrhotic tissues (HBV or HCV infection) and higher HCC by Pearson correlation coefficient and our programming, respectively, as shown in Figure 1 and Table S2.

Mutual relationships of novel *BRCA1*-activated (Pearson ≥0.25) and -inhibited (Pearson ≤−0.25) different complete and uncomplete networks were computed between lower no-tumor hepatitis/cirrhotic tissues (HBV or HCV infection) and higher HCC by scatterplot (matrix) of linear regression and our programming, respectively, as shown in Figure 2 and Table S3.

Novel *BRCA1*-activated (Pearson ≥0.25) and -inhibited (Pearson ≤−0.25) different complete and uncomplete networks including autocorrelations were constructed between lower no-tumor hepatitis/cirrhotic tissues (HBV or HCV infection) and higher HCC by GRNInfer and our programming, respectively, as shown in Figure 3 and Table S4.

Terms and occurrence numbers of GO (Cellular Component, Molecular Function, Biological Process), KEGG, GenMAPP, BioCarta, and disease in novel *BRCA1*-activated (Pearson ≥0.25) and -inhibited (Pearson ≤−0.25) different complete and uncomplete networks were identified between lower no-tumor hepatitis/cirrhotic tissues (HBV or HCV infection) and higher HCC by MAS 3.0 and our programming, respectively, as shown in Figure 4 and Table S5.

DISCUSSION

BRCA1-ACTIVATED INFLAMMATION NETWORK IN NO-TUMOR HEPATITIS/CIRRHOTIC TISSUES (HBV OR HCV INFECTION)

BRCA1-activated different complete and uncomplete networks were identified in lower no-tumor hepatitis/cirrhotic tissues (HBV or HCV infection) (compared with higher HCC) by Pearson and GRNInfer (Fig. 1A,B and Table S2). This result was verified by the corresponding scatter matrix (Fig. 2A,B and Table S3). *BRCA1*-stimulated different complete network was constructed with *IRF5*, *KLRC3* (Fig. 3A and Table S4) and the corresponding uncomplete network with *SLC4A3*, *MCM2*, *AMELY*, *SEMA3B*, *KIAA0513*, *GRM1*, *DDX10*, *C9orf127*, *RNF185*, *MYH6*, *HOXD4*, *TP53I11*, *HMGB2*, *LGALS3*, *KCTD2*, *FGF9*, *ISG20*, *MAP2K6*, *STX1A*, *MS4A2* (Fig. 3B and Table S4). We proposed mainly that *BRCA1*-stimulated different network contained *BRCA1* activation with integral to membrane killer cell lectin-like receptor C to nucleus interferon regulatory factor 5-induced inflammation in lower no-tumor hepatitis/cirrhotic tissues (HBV or HCV infection) by GO, KEGG, GenMAPP, BioCarta, and disease database integration (Fig. 4A,B and Table S5). This hypothesis was verified by the corresponding uncomplete network in no-tumor hepatitis/cirrhotic tissues (HBV or HCV infection) and *BRCA1*-inhibited inflammation network in HCC. References also supported our hypothesis. Such as, NKG2-C type II integral membrane protein is a protein that in humans is encoded by the KLRC2 gene [Plougastel and Trowsdale, 1998]. Natural killer (NK) cells are lymphocytes that can mediate lysis of certain tumor cells and virus-infected cells without previous activation. They can also regulate specific humoral and cell-mediated immunity. NK cells preferentially express several calcium-dependent (C-type) lectins, which have been implicated in the regulation of NK cell function. The group, designated KLRC (NKG2) are expressed primarily in natural killer (NK) cells and encodes a family of transmembrane proteins characterized by a type II membrane orientation (extracellular C terminus) and the presence of a C-type lectin domain. The KLRC (NKG2) gene family is located within the NK complex, a region that contains several C-type lectin genes preferentially expressed on NK cells (http://en.wikipedia.org/wiki/KLRC2).

BRCA1-INHIBITED GROWTH NETWORK IN NO-TUMOR HEPATITIS/CIRRHOTIC TISSUES (HBV OR HCV INFECTION)

BRCA1-inhibited different complete and uncomplete networks were identified in lower no-tumor hepatitis/cirrhotic tissues (HBV or HCV infection) (compared with higher HCC) by Pearson and GRNInfer (Fig. 1C,D and Table S2). This result was verified by the corresponding scatter matrix (Fig. 2C,D and Table S3). *BRCA1*-inhibited different complete network was constructed with *ROBO1*, *VCAN* (Fig. 3C and Table S4) and the corresponding uncomplete network with *GPSM2*, *PTTG1*, *ACTG2*, *ESM1*, *CCL20*, *CTHRC1* (Fig. 3D and Table S4). We proposed mainly that *BRCA1*-inhibited different network participated in *BRCA1* repression with matrix roundabout axon guidance receptor homolog 1 to plasma membrane versican-induced growth in lower no-tumor hepatitis/cirrhotic tissues (HBV or HCV infection) by GO, KEGG, GenMAPP, BioCarta, and disease database integration (Fig. 4C,D and Table S5). This hypothesis was verified by the corresponding uncomplete network in no-tumor hepatitis/cirrhotic tissues (HBV or HCV infection) and *BRCA1*-activated growth network

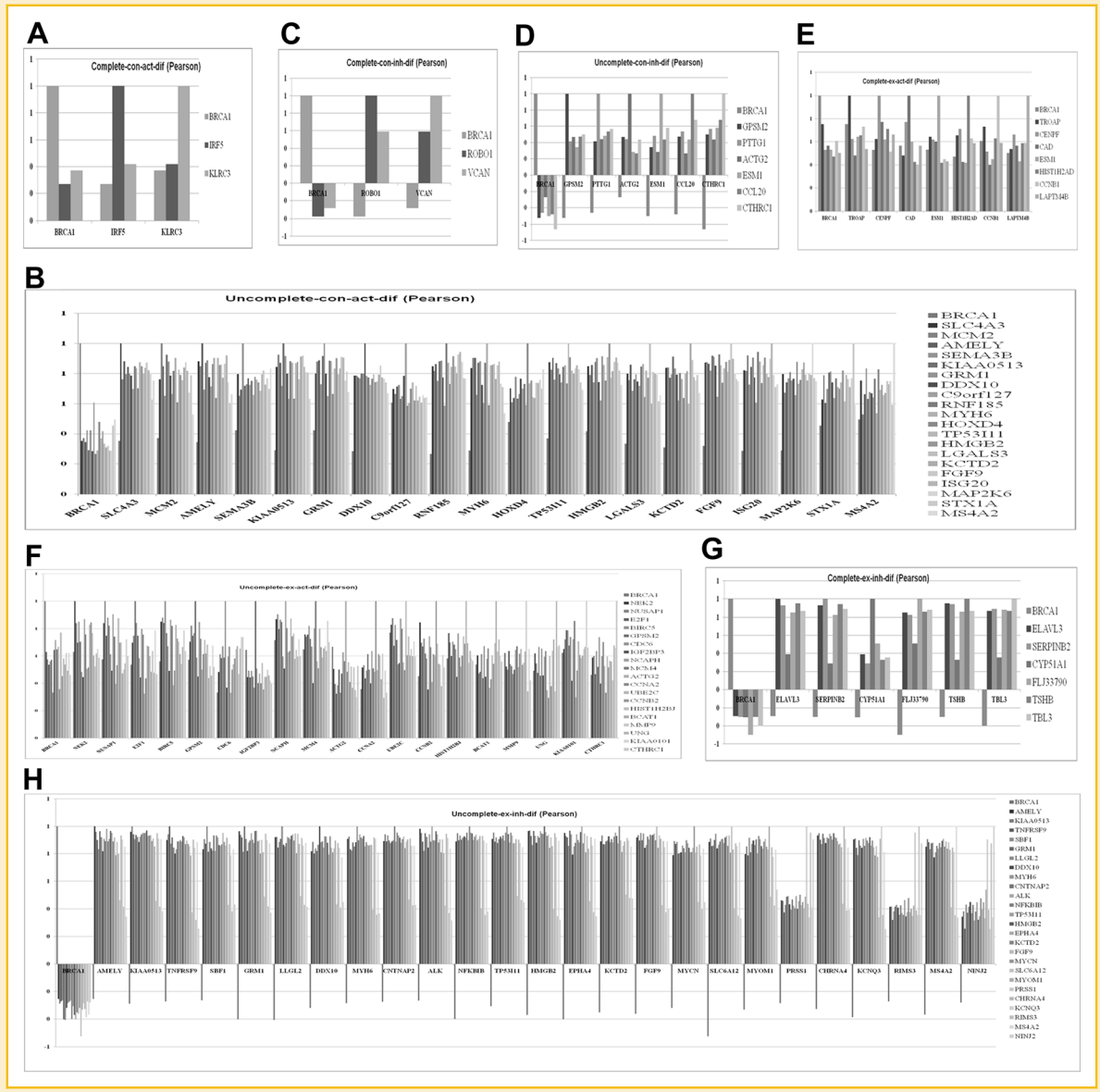

Fig. 1. Vertical bars quantification charts of *BRCA1*-activated and -inhibited different networks by Pearson and our programming. A: Complete and (B) uncomplete *BRCA1*-activated different network in lower expression of no-tumor hepatitis/cirrhotic tissues (HBV or HCV infection) (compared with higher HCC), n = 25. C: Complete and (D) uncomplete *BRCA1*-inhibited different network in lower no-tumor hepatitis/cirrhotic tissues (HBV or HCV infection) (compared with higher HCC), n = 25. E: Complete and (F) uncomplete *BRCA1*-activated different network in higher HCC (compared with lower no-tumor hepatitis/cirrhotic tissues (HBV or HCV infection)), n = 25. G: Complete and (H) uncomplete *BRCA1*-inhibited different network in higher HCC (compared with lower no-tumor hepatitis/cirrhotic tissues (HBV or HCV infection)), n = 25. Black arrow represents as activated relationship and empty circle as inhibited relationship. con, no-tumor hepatitis/cirrhotic tissues (HBV or HCV infection); ex, HCC; act, activation; inh, inhibition; dif, different.

in HCC. References also supported our hypothesis. Such as, Roundabout homolog 1 is a protein that in humans is encoded by the *ROBO1* gene [Kidd et al., 1998; Sundaresan et al., 1998]. Bilateral symmetric nervous systems have special midline structures that establish a partition between the two mirror image halves. Some axons project toward and across the midline in response to long-range chemoattractants emanating from the midline. In Drosophila, the roundabout gene, a member of the immunoglobulin gene superfamily, encodes an integral membrane protein that is both an axon guidance receptor and a cell adhesion receptor. This receptor is involved in the decision by axons to cross the central nervous system midline. The protein encoded by this gene is structurally similar to the Drosophila roundabout protein. Two transcript variants encoding different isoforms have been found for this gene. *ROBO1* was implicated in communication disorder based on a Finnish pedigree with severe dyslexia. Analyses revealed a translocation had occurred disrupting *ROBO1* [Hannula-Jouppi et al., 2005]. Study of the phonological memory component of the language acquisition system

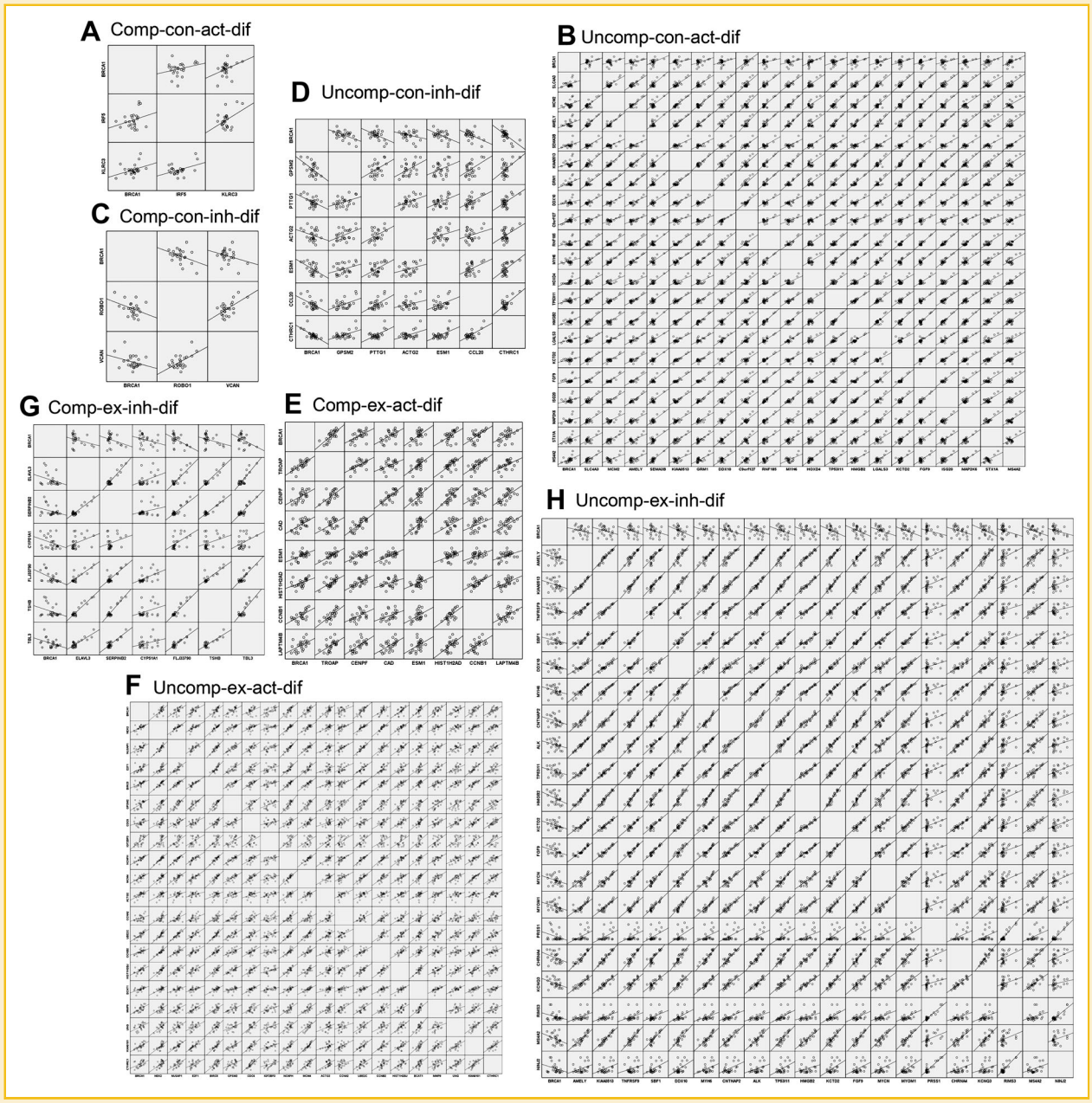

Fig. 2. The mutual relationships of *BRCA1*-activated and -inhibited different networks by scatterplot (matrix) and our programming. A: Complete and (B) uncomplete *BRCA1*-activated different network in lower expression of no-tumor hepatitis/cirrhotic tissues (HBV or HCV infection) (compared with higher HCC), n = 25. C: Complete and (D) uncomplete *BRCA1*-inhibited different network in lower no-tumor hepatitis/cirrhotic tissues (HBV or HCV infection) (compared with higher HCC), n = 25. E: Complete and (F) uncomplete *BRCA1*-activated different network in higher HCC (compared with of no-tumor hepatitis/cirrhotic tissues (HBV or HCV infection)), n = 25. G: Complete and (H) uncomplete *BRCA1*-inhibited different network in higher HCC (compared with lower no-tumor hepatitis/cirrhotic tissues (HBV or HCV infection)), n = 25. Black arrow represents as activated relationship and empty circle as inhibited relationship. Comp, complete; Uncomp, uncomplete; con, no-tumor hepatitis/cirrhotic tissues (HBV or HCV infection); ex, HCC; act, activation; inh, inhibition; dif, different.

suggests that *ROBO1* polymorphisms are associated with functioning in this system [Bates et al., 2011] (http://en.wikipedia.org/wiki/ROBO1).

BRCA1-STIMULATED GROWTH NETWORK IN HCC

BRCA1-activated different complete and uncomplete networks were identified in higher HCC (compared with lower no-tumor hepatitis/cirrhotic tissues (HBV or HCV infection)) by Pearson and GRNInfer (Fig. 1E,F and Table S2). This result was verified by the corresponding scatter matrix (Fig. 2E,F and Table S3). *BRCA1*-stimulated different complete network was constructed with *TROAP*, *CENPF*, *CAD*, *ESM1*, *HIST1H2AD*, *CCNB1*, *LAPTM4B* (Fig. 3E and Table S4) and the corresponding uncomplete network with *NEK2*, *NUSAP1*, *E2F1*, *BIRC5*, *GPSM2*, *CDC6*, *IGF2BP3*, *NCAPH*, *MCM4*, *ACTG2*, *CCNA2*, *UBE2C*, *CCNB2*, *HIST1H2BJ*, *BCAT1*, *MMP9*, *UNG*, *KIAA0101*, *CTHRC1* (Fig. 3F and Table S4). We proposed mainly that *BRCA1*-

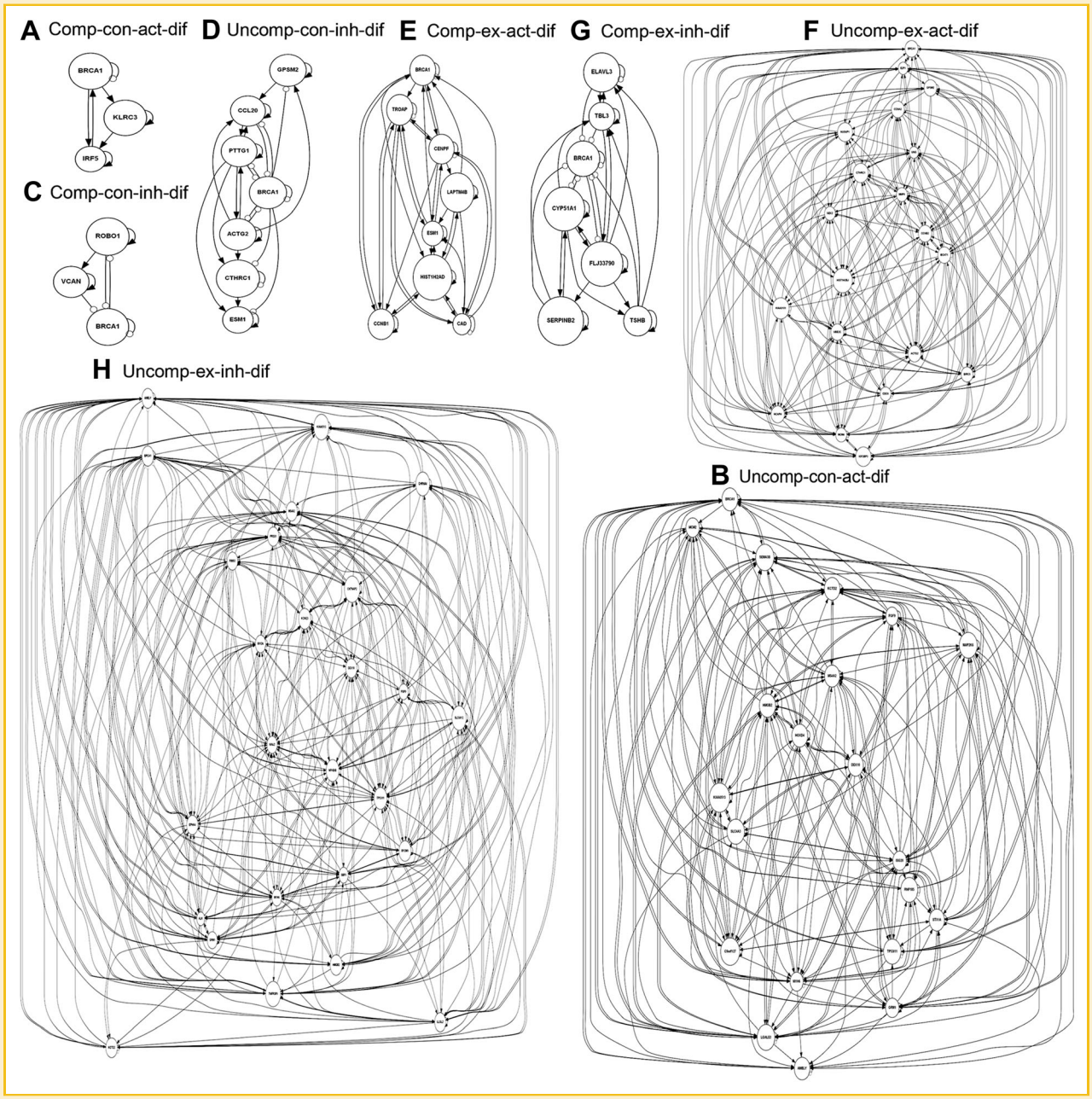

Fig. 3. *BRCA1*-activated and -inhibited different directionality networks by GRNInfer and our programming. A: Complete and (B) uncomplete *BRCA1*-activated different network in lower expression of no-tumor hepatitis/cirrhotic tissues (HBV or HCV infection) (compared with higher HCC), n = 25. C: Complete and (D) uncomplete *BRCA1*-inhibited different network in lower no-tumor hepatitis/cirrhotic tissues (HBV or HCV infection) (compared with higher HCC), n = 25. E: Complete and (F) uncomplete *BRCA1*-activated different network in higher HCC (compared with lower no-tumor hepatitis/cirrhotic tissues (HBV or HCV infection)), n = 25. G: Complete and (H) uncomplete *BRCA1*-inhibited different network in higher HCC (compared with lower no-tumor hepatitis/cirrhotic tissues (HBV or HCV infection)), n = 25. Black arrow represents as activated relationship and empty circle as inhibited relationship. Comp, complete; Uncomp, uncomplete; con, no-tumor hepatitis/cirrhotic tissues (HBV or HCV infection); ex, HCC; act, activation; inh, inhibition; dif, different.

stimulated different network was involved in *BRCA1* activation with endothelium-specific to lysosomal transmembrane and carbamoyl synthetase to tastin, histone cluster and cyclin-induced growth in higher HCC by GO, KEGG, GenMAPP, BioCarta, and disease database integration (Fig. 4E,F and Table S5). This hypothesis was verified by the corresponding uncomplete network in HCC and *BRCA1*-inhibited growth network in no-tumor hepatitis/cirrhotic tissues (HBV or HCV infection). References also supported our hypothesis. Such as, lysosomal-associated transmembrane protein 4B is a protein that in humans is encoded by the *LAPTM4B* gene. *LAPTM4B* protein contains a lysosome localization motif and localizes on late endosomes and lysosomes. Increased expression of *LAPTM4B* has

Fig. 4. Terms and occurrence numbers of GO (Cellular Component, Molecular Function, Biological Process), KEGG, GenMAPP, BioCarta, and Disease by MAS 3.0 and our programming. A: Complete and (B) uncomplete *BRCA1*-activated different network in lower expression of no-tumor hepatitis/cirrhotic tissues (HBV or HCV infection) (compared with higher HCC), n = 25. C: Complete and (D) uncomplete *BRCA1*-inhibited different network in lower no-tumor hepatitis/cirrhotic tissues (HBV or HCV infection) (compared with higher HCC), n = 25. E: Complete and (F) uncomplete *BRCA1*-activated different network in higher HCC (compared with lower no-tumor hepatitis/cirrhotic tissues (HBV or HCV infection)), n = 25. G: Complete and (H) uncomplete *BRCA1*-inhibited different network in higher HCC (compared with lower no-tumor hepatitis/cirrhotic tissues (HBV or HCV infection)), n = 25. Black arrow represents as activated relationship and empty circle as inhibited relationship. Comp, complete; Uncomp, uncomplete; con, no-tumor hepatitis/cirrhotic tissues (HBV or HCV infection); ex, HCC; act, activation; inh, inhibition; dif, different.

been found in breast, liver, lung, ovarian, uterine, gastric cancers. Elevated *LAPTM4B* level contributes to chemotherapy resistance in breast cancer. It was found that overexpression of *LAPTM4B* causes anthracyclines (doxorubicin, daunorubicin, and epirubicin) resistance by retaining drug in the cytoplasm and decreasing nuclear localization of drug and drug induced DNA damage [Li et al., 2010]. *LAPTM4B* also promotes autophagy, a cell survival mechanism mediated by lysosomes. *LAPTM4B* promotes autophagy and renders tumor cells resistant to metabolic and genotoxic stress and results in more rapid tumor growth [Li et al., 2011]. Based on these findings, *LAPTM4B* can be utilized to be a therapeutic target to prevent chemotherapy resistance or a marker to identify the patients who will not benefit from anthracyclines [Li et al., 2010] (http://en.wikipedia.org/wiki/LAPTM4B).

BRCA1-REPRESSED INFLAMMATION NETWORK IN HCC

BRCA1-inhibited different complete and uncomplete networks were identified in higher HCC (compared with lower no-tumor hepatitis/cirrhotic tissues (HBV or HCV infection)) by Pearson and GRNInfer (Fig. 1G,H and Table S2). This result was verified by the corresponding scatter matrix (Fig. 2G,H and Table S3). *BRCA1*-inhibited different complete network was constructed with *ELAVL3*, *SERPINB2*, *CYP51A1*, *FLJ33790*, *TSHB*, *TBL3* (Fig. 3G and Table S4) and the corresponding uncomplete network with *AMELY*, *KIAA0513*, *TNFRSF9*, *SBF1*, *GRM1*, *LLGL2*, *DDX10*, *MYH6*, *CNTNAP2*, *ALK*, *NFKBIB*, *TP53I11*, *HMGB2*, *EPHA4*, *KCTD2*, *FGF9*, *MYCN*, *SLC6A12*, *MYOM1*, *PRSS1*, *CHRNA4*, *KCNQ3*, *RIMS3*, *MS4A2*, *NINJ2* (Fig. 3H and Table S4). We proposed mainly that *BRCA1*-inhibited different network included *BRCA1* repression with ovalbumin, thyroid stimulating hormone beta and Hu antigen C to cytochrome P450 to transducin-induced inflammation in higher HCC by GO, KEGG, GenMAPP, BioCarta, and disease database integration (Fig. 4G,H and Table S5). This hypothesis was verified by the corresponding uncomplete network in HCC and *BRCA1*-activated inflammation network in no-tumor hepatitis/cirrhotic tissues (HBV or HCV infection). References also supported our hypothesis. Such as, Lanosterol 14 α-demethylase (or CYP51A1, P45014DM) is a cytochrome P450 (family 51, subfamily A, polypeptide 1) enzyme that converts lanosterol to cholesterol. It is a target for antifungal drugs, inhibiting the production of ergosterol. Over-expression of CYP51A1 can lead to resistance to these antifungals [Vanden Bossche et al., 1998]. Azole fungicides are demethylase inhibitors that inhibit CYP51 activity [Mullins et al., 2011]. CYP51 is a cytochrome P450 that catalyses the oxidative removal of the 14α-methyl group of lanosterol or eburicol in yeasts and fungi—an essential step in the production of sterols [Mullins et al., 2011]. Azoles bind as the sixth ligand to the haem in CYP51 via the unprotonated N atom thus occupying the active site and acting as non-competitive inhibitors [Mullins et al., 2011] (http://en.wikipedia.org/wiki/CYP51A1).

BRCA1 NETWORKS AUTOCORRELATIONS

In *BRCA1*-stimulated different complete network of lower no-tumor hepatitis/cirrhotic tissues (HBV or HCV infection) (compared with higher HCC), there is *IRF5* auto-activation including upstream *KLRC3*, *BRCA1* downstream *BRCA1*; There is *KLRC3* auto-activation including upstream *BRCA1* downstream *IRF5* by GRNInfer (Fig. 3A and Table S4). Thus, our results reflected the stimulation of *IRF5* upstream; *KLRC3* the same in no-tumor hepatitis/cirrhotic tissues. There is *BRCA1* auto-inhibition containing upstream *IRF5* downstream *KLRC3*, *IRF5* by GRNInfer (Fig. 3A and Table S4). Thus, our results reflected the repression of *BRCA1* upstream molecular numbers in no-tumor hepatitis/cirrhotic tissues.

In *BRCA1*-inhibited different complete network of lower no-tumor hepatitis/cirrhotic tissues (HBV or HCV infection) (compared with higher HCC), there is *ROBO1* auto-activation including upstream *BRCA1* downstream *VCAN*, *BRCA1*; There is *VCAN* auto-activation including upstream *ROBO1* downstream *BRCA1* by GRNInfer (Fig. 3C and Table S4). Thus, our results reflected the stimulation of *ROBO1* downstream; *VCAN* the same in no-tumor hepatitis/cirrhotic tissues. There is *BRCA1* auto-inhibition containing upstream *ROBO1*, *VCAN* downstream *ROBO1* by GRNInfer (Fig. 3C and Table S4). Thus, our results reflected the repression of *BRCA1* downstream molecular numbers in no-tumor hepatitis/cirrhotic tissues.

In *BRCA1*-stimulated different complete network of higher HCC (compared with lower no-tumor hepatitis/cirrhotic tissues (HBV or HCV infection)), there is *ESM1* auto-activation including upstream *TROAP*, *CENPF*, *CAD*, *HIST1H2AD*, *LAPTM4B* downstream *TROAP*, *BRCA1*, *CENPF*, *HIST1H2AD*; There is *HIST1H2AD* auto-activation including upstream *BRCA1*, *CAD*, *ESM1*, *CCNB1*, *LAPTM4B* downstream *CAD*, *ESM1*, *CCNB1*, *LAPTM4B*; There is *CCNB1* auto-activation including upstream *BRCA1*, *TROAP*, *CENPF*, *HIST1H2AD* downstream *TROAP*, *BRCA1*, *HIST1H2AD*; There is *LAPTM4B* auto-activation including upstream *CENPF*, *HIST1H2AD* downstream *BRCA1*, *CAD*, *ESM1*, *HIST1H2AD* by GRNInfer (Fig. 3E and Table S4). Thus, our results reflected the stimulation of *CCNB1*, *HIST1H2AD*, *ESM1* upstream; *LAPTM4B* downstream in HCC. There is *BRCA1* auto-inhibition containing upstream *CENPF*, *CAD*, *ESM1*, *CCNB1*, *LAPTM4B* downstream *CENPF*, *HIST1H2AD*, *CCNB1*, *TROAP*; There is *TROAP* auto-inhibition containing upstream *CENPF*, *CAD*, *ESM1*, *CCNB1*, *BRCA1* downstream *CENPF*, *CAD*, *ESM1*, *CCNB1*; There is *CENPF* auto-inhibition containing upstream *BRCA1*, *TROAP*, *CAD*, *ESM1* downstream *TROAP*, *BRCA1*, *CAD*, *ESM1*, *CCNB1*, *LAPTM4B*; There is *CAD* auto-inhibition containing upstream *TROAP*, *CENPF*, *HIST1H2AD*, *LAPTM4B* downstream *TROAP*, *BRCA1*, *CENPF*, *ESM1*, *HIST1H2AD* by GRNInfer (Fig. 3E and Table S4). Thus, our results reflected the repression of *CAD*, *CENPF* upstream; *TROAP*, *BRCA1* downstream molecular numbers in HCC.

In *BRCA1*-inhibited different complete network of higher HCC (compared with lower no-tumor hepatitis/cirrhotic tissues (HBV or HCV infection)), there is *SERPINB2* auto-activation including upstream *CYP51A1*, *FLJ33790* downstream *CYP51A1*, *TBL3*, *BRCA1*; There is *CYP51A1* auto-activation including upstream *SERPINB2*, *FLJ33790*, *BRCA1* downstream *SERPINB2*, *FLJ33790*, *TSHB*, *TBL3*, *BRCA1*; There is *FLJ33790* auto-activation including upstream *CYP51A1*, *TBL3*, *BRCA1* downstream *ELAVL3*, *SERPINB2*, *CYP51A1*, *TSHB*, *TBL3*, *BRCA1*; There is *TSHB* auto-activation including upstream *CYP51A1*, *FLJ33790* downstream *ELAVL3*, *TBL3*, *BRCA1*; There is *TBL3* auto-activation including upstream *SERPINB2*, *CYP51A1*, *FLJ33790*, *TSHB*, *ELAVL3* downstream *ELAVL3*, *FLJ33790*, *BRCA1* by GRNInfer (Fig. 3G and

Table S4). Thus, our results reflected the stimulation of *TBL3* upstream; *TSHB*, *FLJ33790*, *CYP51A1*, *SERPINB2* downstream in HCC. There is *BRCA1* auto-inhibition containing upstream *ELAVL3*, *SERPINB2*, *CYP51A1*, *FLJ33790*, *TSHB*, *TBL3* downstream *CYP51A1*, *FLJ33790*; There is *ELAVL3* auto-inhibition containing upstream *FLJ33790*, *TSHB*, *TBL3* downstream *BRCA1*, *TBL3* by GRNInfer (Fig. 3G and Table S4). Thus, our results reflected the repression of *ELAVL3*, *BRCA1* downstream molecular numbers in HCC.

SUMMARY

As visualized by GO, KEGG, GenMAPP, BioCarta, and disease database integration, we proposed mainly that *BRCA1*-stimulated different complete network was involved in *BRCA1* activation with integral to membrane killer cell lectin-like receptor C to nucleus interferon regulatory factor 5-induced inflammation, whereas the corresponding inhibited network participated in *BRCA1* repression with matrix roundabout axon guidance receptor homolog 1 to plasma membrane versican-induced growth in lower no-tumor hepatitis/cirrhotic tissues (HBV or HCV infection). However, *BRCA1*-stimulated network contained *BRCA1* activation with endothelium-specific to lysosomal transmembrane and carbamoyl synthetase to tastin, histone cluster and cyclin-induced growth, whereas the corresponding inhibited different complete network included *BRCA1* repression with ovalbumin, thyroid stimulating hormone beta and Hu antigen C to cytochrome P450 to transducin-induced inflammation in higher HCC. Our *BRCA1* different networks were verified by *BRCA1*-activated or -inhibited complete and uncomplete networks within and between no-tumor hepatitis/cirrhotic tissues (HBV or HCV infection) or (and) HCC.

REFERENCES

Bates TC, Luciano M, Medland SE, Montgomery GW, Wright MJ, Martin NG. 2011. Genetic variance in a component of the language acquisition device: ROBO1 polymorphisms associated with phonological buffer deficits. Behav Genet 41:50–57.

Boulton SJ. 2006. Cellular functions of the BRCA tumour-suppressor proteins. Biochem Soc Trans 34:633–645.

Hannula-Jouppi K, Kaminen-Ahola N, Taipale M, Eklund R, Nopola-Hemmi J, Kaariainen H, Kere J. 2005. The axon guidance receptor gene ROBO1 is a candidate gene for developmental dyslexia. PLoS Genet 1:e50.

Huang J, Wang L, Jiang M, Lin H, Qi L, Diao H. 2012. PTHLH coupling upstream negative regulation of fatty acid biosynthesis and Wnt receptor signal to downstream peptidase activity-induced apoptosis network in human hepatocellular carcinoma by systems-theoretical analysis. J Recept Signal Transduct Res 32:250–256.

Huang J, Wang L, Jiang M, Zheng X. 2010. Interferon α-inducible protein 27 computational network construction and comparison between the frontal cortex of hiv encephalitis (HIVE) and HIVE-control patients. Open Genomics J 3:1–8.

Huang JX, Wang L, Jiang MH. 2011. TNFRSF11B computational development network construction and analysis between frontal cortex of HIV encephalitis (HIVE) and HIVE-control patients. J Inflamm (Lond) 7:50.

Kidd T, Brose K, Mitchell KJ, Fetter RD, Tessier-Lavigne M, Goodman CS, Tear G. 1998. Roundabout controls axon crossing of the CNS midline and defines a novel subfamily of evolutionarily conserved guidance receptors. Cell 92: 205–215.

Li Y, Zhang Q, Tian R, Wang Q, Zhao JJ, Iglehart JD, Wang ZC, Richardson AL. 2011. Lysosomal transmembrane protein LAPTM4B promotes autophagy and tolerance to metabolic stress in cancer cells. Cancer Res 71:7481–7489.

Li Y, Zou L, Li Q, Haibe-Kains B, Tian R, Desmedt C, Sotiriou C, Szallasi Z, Iglehart JD, Richardson AL, Wang ZC. 2010. Amplification of LAPTM4B and YWHAZ contributes to chemotherapy resistance and recurrence of breast cancer. Nat Med 16:214–218.

Lin H, Wang L, Jiang M, Huang J, Qi L. 2012. P-glycoprotein (ABCB1) inhibited network of mitochondrion transport along microtubule and BMP signal-induced cell shape in chimpanzee left cerebrum by systems-theoretical analysis. Cell Biochem Funct 30:582–587.

Mullins JG, Parker JE, Cools HJ, Togawa RC, Lucas JA, Fraaije BA, Kelly DE, Kelly SL. 2011. Molecular modelling of the emergence of azole resistance in Mycosphaerella graminicola. PLoS ONE 6:e 20973.

Plougastel B, Trowsdale J. 1998. Sequence analysis of a 62-kb region overlapping the human KLRC cluster of genes. Genomics 49:193–199.

Storey JD. 2002. A direct approach to false discovery rates. J Roy Stat Soc Ser B 64:479–498.

Sun L, Wang L, Jiang M, Huang J, Lin H. 2011. Glycogen debranching enzyme 6 (AGL), enolase 1 (ENOSF1), ectonucleotide pyrophosphatase 2 (ENPP2_1), glutathione S-transferase 3 (GSTM3_3) and mannosidase (MAN2B2) metabolism computational network analysis between chimpanzee and human left cerebrum. Cell Biochem Biophys 61:493–505.

Sun Y, Wang L, Jiang M, Huang J, Liu Z, Wolfl S. 2010. Secreted phosphoprotein 1 upstream invasive network construction and analysis of lung adenocarcinoma compared with human normal adjacent tissues by integrative biocomputation. Cell Biochem Biophys 56:59–71.

Sundaresan V, Roberts I, Bateman A, Bankier A, Sheppard M, Hobbs C, Xiong J, Minna J, Latif F, Lerman M, Rabbitts P. 1998. The DUTT1 gene, a novel NCAM family member is expressed in developing murine neural tissues and has an unusually broad pattern of expression. Mol Cell Neurosci 11:29–35.

Vanden Bossche H, Dromer F, Improvisi I, Lozano-Chiu M, Rex JH, Sanglard D. 1998. Antifungal drug resistance in pathogenic fungi. Med Mycol 36 (Suppl1):119–128.

Wang H, Shao N, Ding QM, Cui J, Reddy ES, Rao VN. 1997. BRCA1 proteins are transported to the nucleus in the absence of serum and splice variants BRCA1a, BRCA1b are tyrosine phosphoproteins that associate with E2F, cyclins and cyclin dependent kinases. Oncogene 15:143–157.

Wang L, Huang J, Jiang M. 2011a. CREB5 computational regulation network construction and analysis between frontal cortex of HIV encephalitis (HIVE) and HIVE-control patients. Cell Biochem Biophys 60:199–207.

Wang L, Huang J, Jiang M. 2011b. RRM2 computational phosphoprotein network construction and analysis between no-tumor hepatitis/cirrhotic liver tissues and human hepatocellular carcinoma (HCC). Cell Physiol Biochem 26:303–310.

Wang L, Huang J, Jiang M, Lin H. 2012a. Signal transducer and activator of transcription 2 (STAT2) metabolism coupling postmitotic outgrowth to visual and sound perception network in human left cerebrum by biocomputation. J Mol Neurosci 47:649–658.

Wang L, Huang J, Jiang M, Lin H. 2012b. Tissue-specific transplantation antigen P35B (TSTA3) immune response-mediated metabolism coupling cell cycle to postreplication repair network in no-tumor hepatitis/cirrhotic tissues (HBV or HCV infection) by biocomputation. Immunol Res 52:258–268.

Wang L, Huang J, Jiang M, Lin H, Qi L, Diao H. 2012c. Activated PTHLH coupling feedback phosphoinositide to g-protein receptor signal-induced cell adhesion network in human hepatocellular carcinoma by systems-theoretic analysis. ScientificWorldJournal 2012:428979.

Wang L, Huang J, Jiang M, Lin H, Qi L, Diao H. 2012d. Inhibited PTHLH downstream leukocyte adhesion-mediated protein amino acid N-linked glycosylation coupling Notch and JAK-STAT cascade to iron-sulfur cluster assembly-induced aging network in no-tumor hepatitis/cirrhotic tissues (HBV or HCV infection) by systems-theoretical analysis. Integr Biol (Camb) 4: 1256–1262.

Wang L, Huang J, Jiang M, Sun L. 2011c. MYBPC1 computational phosphoprotein network construction and analysis between frontal cortex of HIV encephalitis (HIVE) and HIVE-control patients. Cell Mol Neurobiol 31:233–241.

Wang L, Huang J, Jiang M, Sun L. 2011d. Survivin (BIRC5) cell cycle computational network in human no-tumor hepatitis/cirrhosis and hepatocellular carcinoma transformation. J Cell Biochem 112:1286–1294.

Wang L, Huang J, Jiang M, Zheng X. 2011e. AFP computational secreted network construction and analysis between human hepatocellular carcinoma (HCC) and no-tumor hepatitis/cirrhotic liver tissues. Tumour Biol 31:417–425.

Wang L, Sun L, Huang J, Jiang M. 2011f. Cyclin-dependent kinase inhibitor 3 (CDKN3) novel cell cycle computational network between human non-malignancy associated hepatitis/cirrhosis and hepatocellular carcinoma (HCC) transformation. Cell Prolif 44:291–299.

Wang L, Sun Y, Jiang M, Zhang S, Wolfl S. 2009a. FOS proliferating network construction in early colorectal cancer (CRC) based on integrative significant function cluster and inferring analysis. Cancer Invest 27: 816–824.

Wang L, Sun Y, Jiang M, Zheng X. 2009b. Integrative decomposition procedure and Kappa statistics for the distinguished single molecular network construction and analysis. J Biomed Biotechnol 2009:726728.

Wang Y, Joshi T, Zhang XS, Xu D, Chen L. 2006. Inferring gene regulatory networks from multiple microarray datasets. Bioinformatics 22:2413–2420.

SUPPORTING INFORMATION

Additional supporting information may be found in the online version of this article at the publisher's web-site.